CIRM(EXT)12

May 1998

A new beam current monitor for the NPL linear accelerator facility.

A J Williams, M R McEwen and D T Burns[†]
Centre for Ionising Radiation Metrology
National Physical Laboratory
Teddington
Middlesex
United Kingdom TW11 0LW

now at Bureau International des Poids et Mesures (BIPM), Paris.

ABSTRACT

A new beam current monitor has been designed and built for the NPL linear accelerator. The output response of the new beam current monitor is relatively free from RF interference: it has a fast rise time of ~10 ns, and is stable enough to be calibrated for absolute charge measurements. The uncertainty on these charge calibrations is estimated to be ± 0.3% (1 σ).

ISSN 1369-6793

National Physical Laboratory
Teddington, Middlesex, UK, TW11 0LW

Approved on behalf of Managing Director, NPL,
by Dr. J B Hunt, Head of Centre, Centre for Ionising Radiation Metrology

CONENTS

TABLES

ILLUSTRATIONS

1 INTRODUCTION

A new Beam Current Monitor (BCM) has been designed and built for the NPL linear accelerator (LINAC). The previous BCM[1] was based on pulse transformer techniques. It was susceptible to RF noise pick-up and its response/rise time was of the order of 100 ns, which was limiting in certain applications. The new BCM is relatively free from RF interference, has a rise time of 10 ns, is three times more sensitive and is stable enough to be calibrated for absolute charge measurements.

The new BCM system is shown schematically in **Figure 1**. Briefly, a toroidal core of supermumetal (higher permeability than standard mumetal) is fixed with its axis coincident with

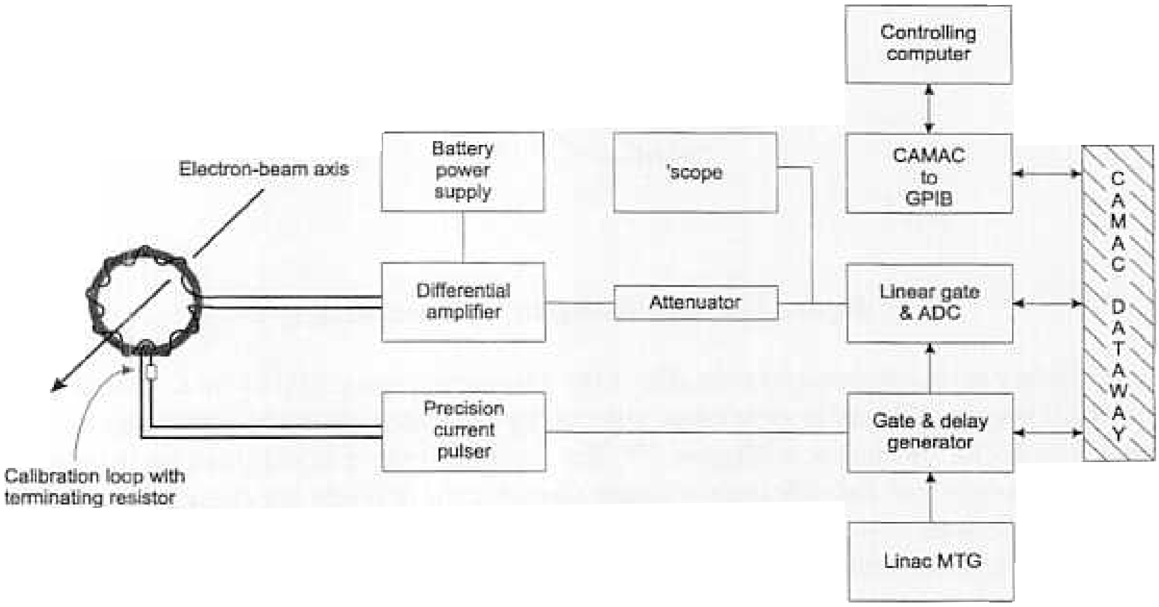

Figure 1 Schematic diagram of the new BCM

the electron beam axis, near the exit window of the accelerator flight tube. The pulsed electron beam current acts as the primary winding of the toroidal transformer. The output signal induced in the secondary winding is fed to the accelerator control room by means of a 100 Ω twin-axial cable. In the control room, a differential amplifier removes any electrical noise pick-up generated in the cable. The output signal from the amplifier is input to a charge sensing ADC gated from the master trigger generator (MTG) of the linac. The ADC output is directly proportional to the electron beam current and can be read on a pulse by pulse basis by a controlling computer. In addition, a single turn calibration loop enables the BCM to be calibrated using a precision pulsed current generator.

2 DESIGN AND CONSTRUCTION

2.1 TOROID AND CASING

The toroid is a Type 13c, made from 0.05 mm supermumetal tape[(a)]. It has an outside diameter of 159 mm, an inside diameter 114 mm and an axial length 25.4 mm, and is supplied in a plastic case.

[(a)] Supplied by Telcon Ltd. (Speciality alloys and components), Napier Way, Crawley, West Sussex, UK.

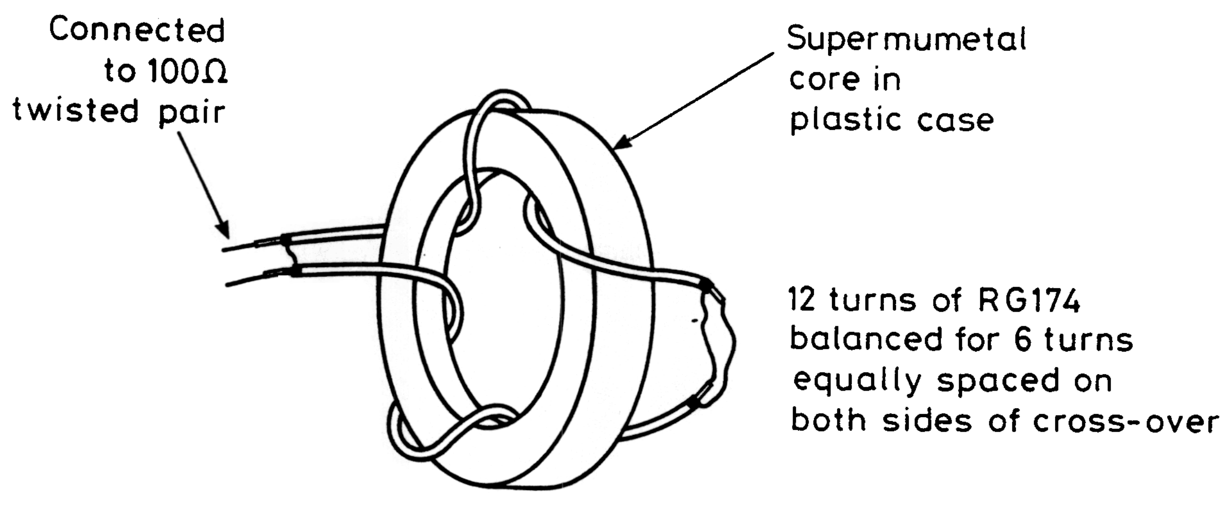

Figure 2 Schematic diagram of toroid winding

The secondary is wound around the outside of the plastic case using RG174 50 Ω coaxial cable[2]. Two equal lengths of the cable were joined together by symmetrically cross-connecting braid and centre conductor as shown in **Figure 2**[(b)]. Six carefully spaced equal turns were wound in opposite directions until the ends came together diametrically opposite the crossover point. Here the two shields were joined. The two centre conductors were twisted together and brought out from the toroid to be soldered to a twin axial bulkhead connector.

This winding arrangement is equivalent to 24 turns of normal wire (as both the shield and centre core of the coax must be considered). There were two reasons for using 50 Ω coaxial cable for the secondary winding, instead of normal wire. Firstly, winding the secondary as described above should eliminate electrical field effects and secondly, winding in this way presents an output impedance of 100 Ω. The secondary winding can therefore be connected directly to a 100 Ω twisted pair coaxial cable for the transfer of the output pulse to the electronics in the accelerator control room, some 12 metres away.

In order to achieve the best signal to noise ratio for the toroidal output, an aluminum casing was designed and built, as shown in **Figure 3** and **Figure 4**. This casing fits over the outside of the beam exit window arrangement and can be easily removed if required. It is isolated from the accelerator earth which is known to be noisy. The signal from the toroid exits the casing via a 100 Ω twin-axial cable connector, to which the cable carrying the pulse to the electronics in the control room is connected. There is also a 50 Ω coaxial cable connector into the toroid casing to allow the entry of a calibration pulse. The calibration circuit is simply a single turn of 0.6 mm insulated wire around the toroid, terminated by a 50 Ω metal film resistor. This allows a calibration current pulse to be used to check the output calibration and stability of the complete BCM system without removing the apparatus from the accelerator, and while the accelerator is still running.

(b) Adapted from Sutter, 1973

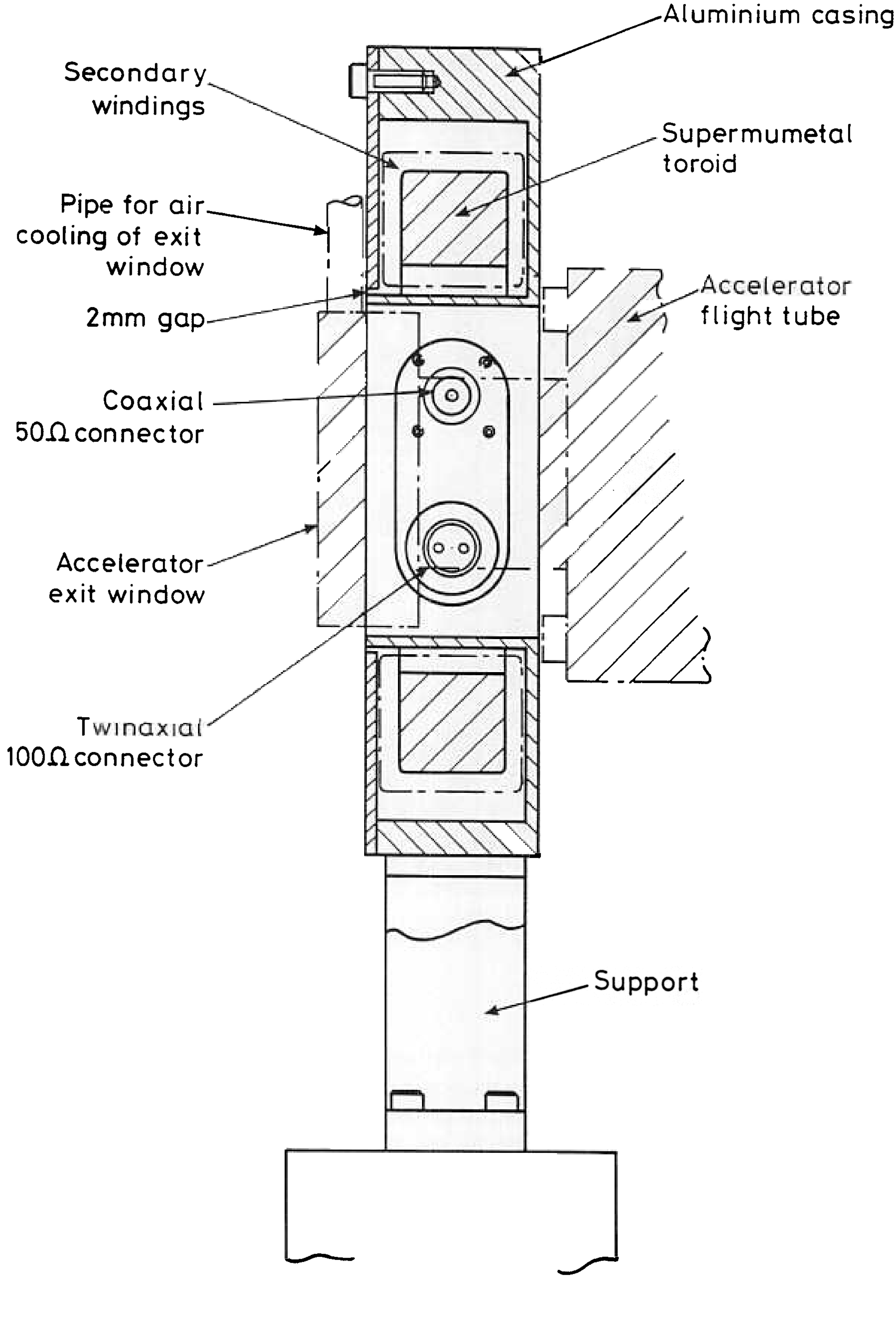

Figure 3 Toroid casing, side view

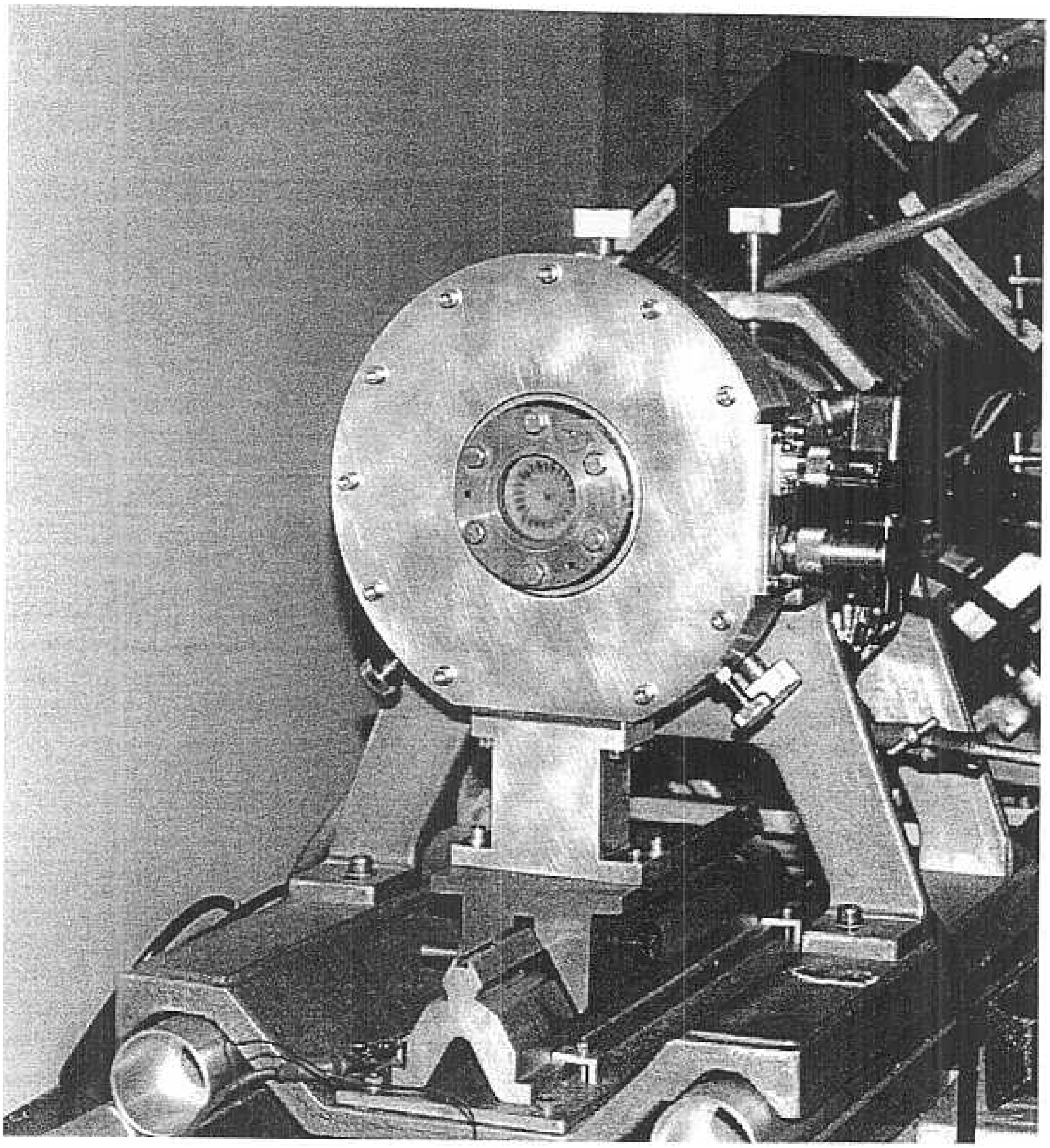

Figure 4 Toroid and casing in situ around the accelerator flight tube

2.2 ELECTRONICS

Having travelled down the connecting cable from the toroid to the control room, the toroid signal is terminated by a 50 Ω metal film resistor on each signal line. The positive and negative pulses from the toroid will normally have picked up some noise in the 12 metre cable run. However, most of this can be removed by subtracting one signal from the other using a differential amplifier, as shown in **Figure 5**[c]. The op-amps used in the construction of the amplifier were Burr-Brown type OPA620KP. All the resistors were precision metal film and each op-amp was by-passed using 10 μF tantalum and 0.1 μF ceramic capacitors. In order to eliminate the possibility of the amplifier oscillating at high frequencies, a printed circuit board was designed

[c] Adapted from Sutter, 1973 and Burr-Brown OPA620 data sheet.

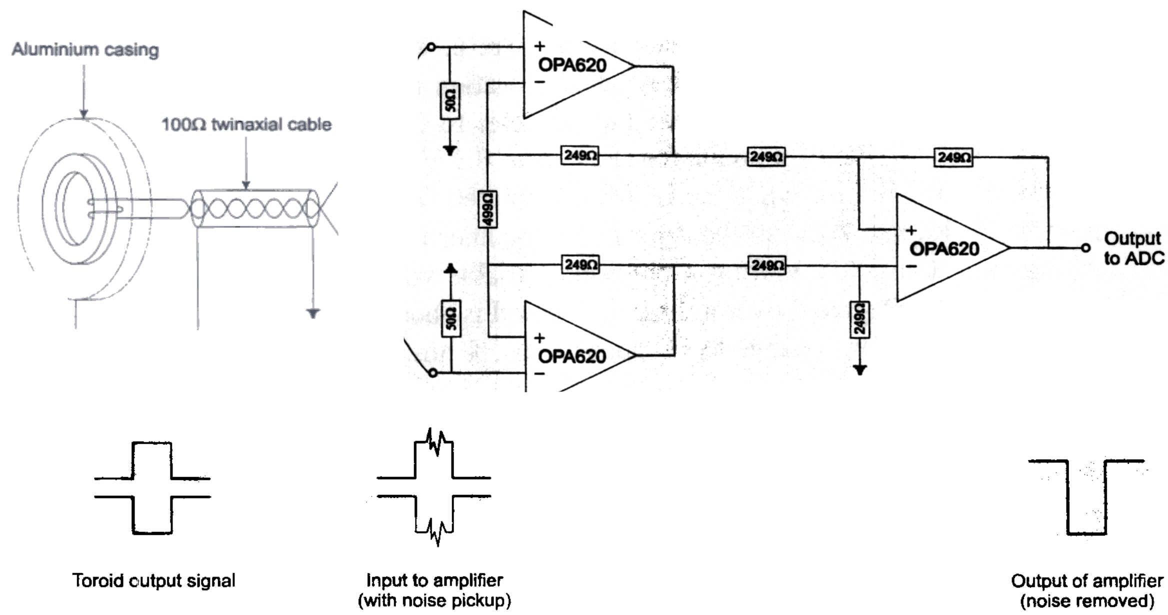

Figure 5 Differential amplifier

and constructed with both sides of the input stage of the amplifier being made as symmetrical as possible. The circuit board also provided a 1 oz copper ground plane: a good ground plane can reduce stray signal pick-up, provide a low resistance, low inductance common return path for signal and power, and can conduct heat from the active circuit package pins into ambient air by convection.

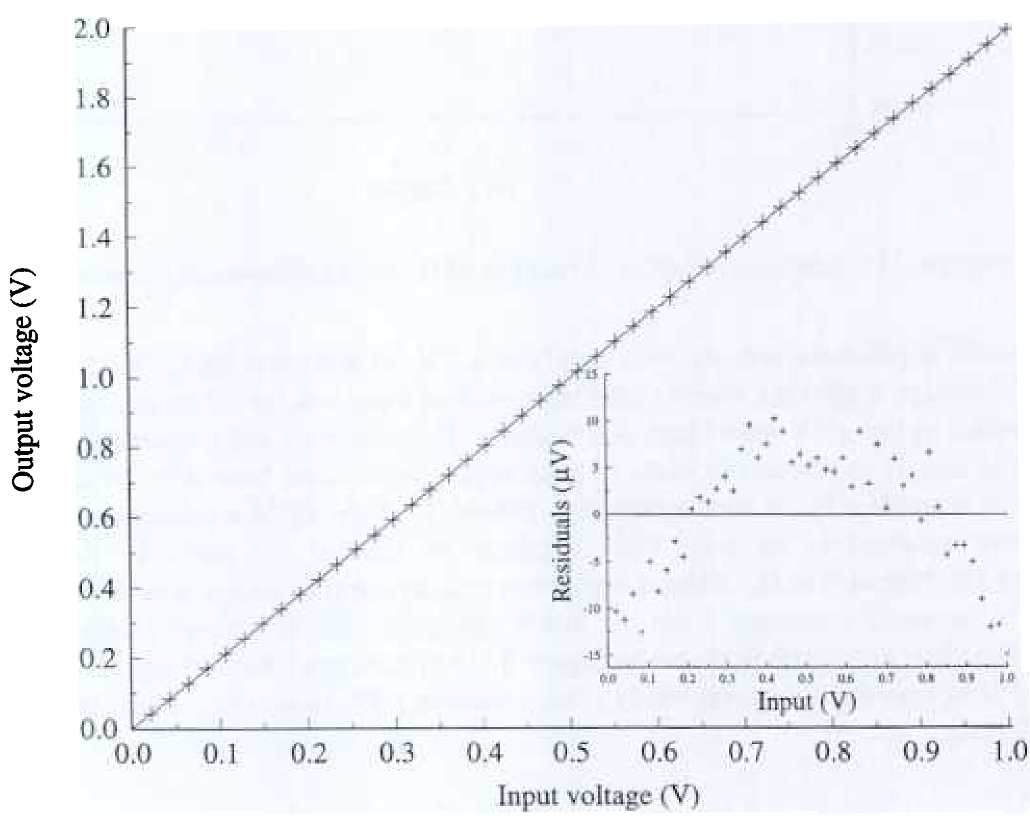

Figure 6 A plot of input volts against output volts for the BCM amplifier

The DC linearity of the amplifier was tested by measuring the output of the system for an input voltage of between 0 and 1 V, as is shown in **Figure 6**, which represents a beam current of between 0 and 240 mA per pulse. The residual deviation from a linear fit of this data is also shown in **Figure 6**. Although this shows the amplifier to be slightly non-linear, the deviation from a straight line fit to the data points for an input of 0.1 V is only 0.01%, and in any case this non-linearity is corrected for when the BCM is calibrated. The output stability of the amplifier was also tested. **Figure 7** shows the drift in the amplifier output over a number of days for a constant input of 0.499808 V from a precision variable voltage supply. The stability of the amplifier as shown in **Figure 7** over a three day period is about ± 0.01% in the worst case. The output of the amplifier may change by as much as 0.05% after a battery recharge.

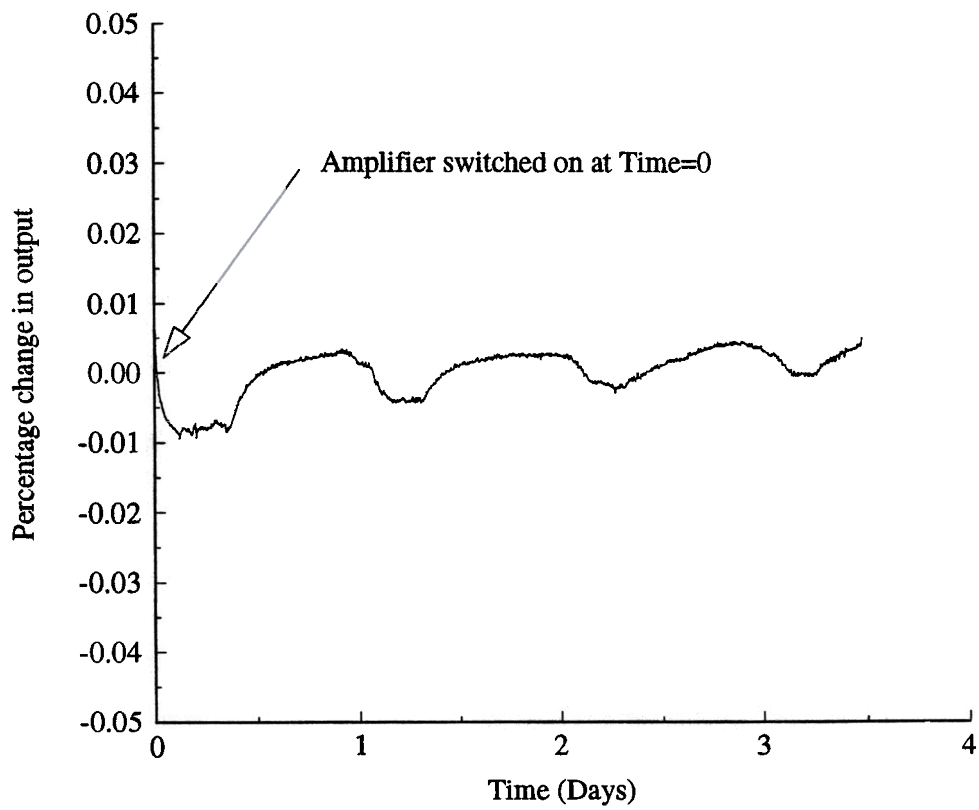

Figure 7 Percentage change in the output of the BCM differential amplifier

The differential amplifier requires a power supply of ± 5 V. This is provided by 7805 (+5 V) and 7905 (-5 V) voltage regulators, which themselves need an input voltage of greater than ± 7.2 V. This is supplied by two 12 V sealed lead-acid batteries. Batteries were used instead of a stepped-down mains supply to isolate the BCM's power supply from mains born interference which is known to be a problem in the accelerator environment. Both the BCM amplifier and the power supply were enclosed in the same EMC shielded 3U KM6-II 19" subrack. The circuitry connecting the batteries to the voltage regulators was arranged in such a way as to allow the batteries to be easily recharged from the mains overnight without removing them from the subrack. The charging circuit is shown in **Figure 8**. The maximum length of time for which the BCM amplifier may be run continuously is approximately $3^1/_2$ days, after which the batteries need recharging.

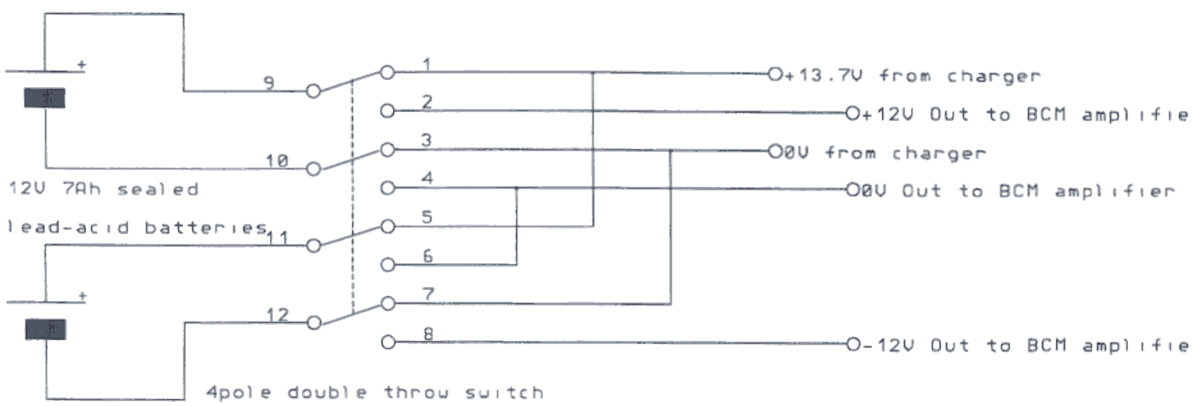

Figure 8 The arrangement of the BCM power supply with battery charging circuitry.

The output of the differential amplifier was connected via a 50 Ω coaxial cable and a 50 Ω switchable attenuator to a gated integrating ADC. (Alternatively, the output pulse can be displayed directly on an oscilloscope with a 50 ohm input impedance). The gated integrating system is the same as that used for the previous BCM. It is centred around a LeCroy Research Systems 2249W Analogue to Digital Converter (ADC). This is a 12-channel 11-bit charge sensing gated integrator, with a resolution of 1 in 2^{11}, i.e. 0.05%, and a full scale reading of a nominal 500 pC. The ADC output is a value between 0 and 2048 representing 0 to 500 pC charge input. The gate (the time period over which the ADC integrates the analogue input signal) is provided by a LeCroy 2323 dual gate generator which is triggered by the linac MTG. The amount of charge in each gated signal pulse from the BCM is measured by the ADC which is in turn is read by a computer using the CAMAC (Computer Automated Measurement And Control) and IEEE-488 standard. Each pulse from the toroid can therefore be measured separately, and the total charge in a run calculated. Pulses for which the output of the BCM amplifier is greater then 500 pC per pulse must be attenuated before entry into the ADC.

3 PERFORMANCE

3 OUTPUT PULSE SHAPE

Figure 9 shows the output of the BCM for a nominal 1 μs test pulse, with rise and fall times of less than 5 ns, 1 μs being the width of a typical linac pulse. The parameters of the *output* pulse are: rise time 6.7 ns, fall time 7.8 ns. The fact that these rise and fall times are very fast means that the BCM can easily resolve the narrowest pulse (20 ns) that the linac can produce. The fractional droop at the end of the output pulse was measured to be about 0.5% per μs. The effect of this droop is to underestimate the amount of charge in the pulse: however, this is taken into account during the calibration procedure. **Figure 10**, **Figure 11**, and **Figure 12** show the output signal of the new BCM for a real beam pulse, the output signal of the old BCM for the same beam pulse, and the output signal collected from an aluminium target placed at the exit window. The rise times of the three systems are 15 ns, 60 ns and 16 ns respectively. From these figures it can be seen that the rise time of the old BCM is too slow to resolve the stepped front edge of the electron pulse, and the new BCM is much less sensitive to electrical interference than the old BCM.

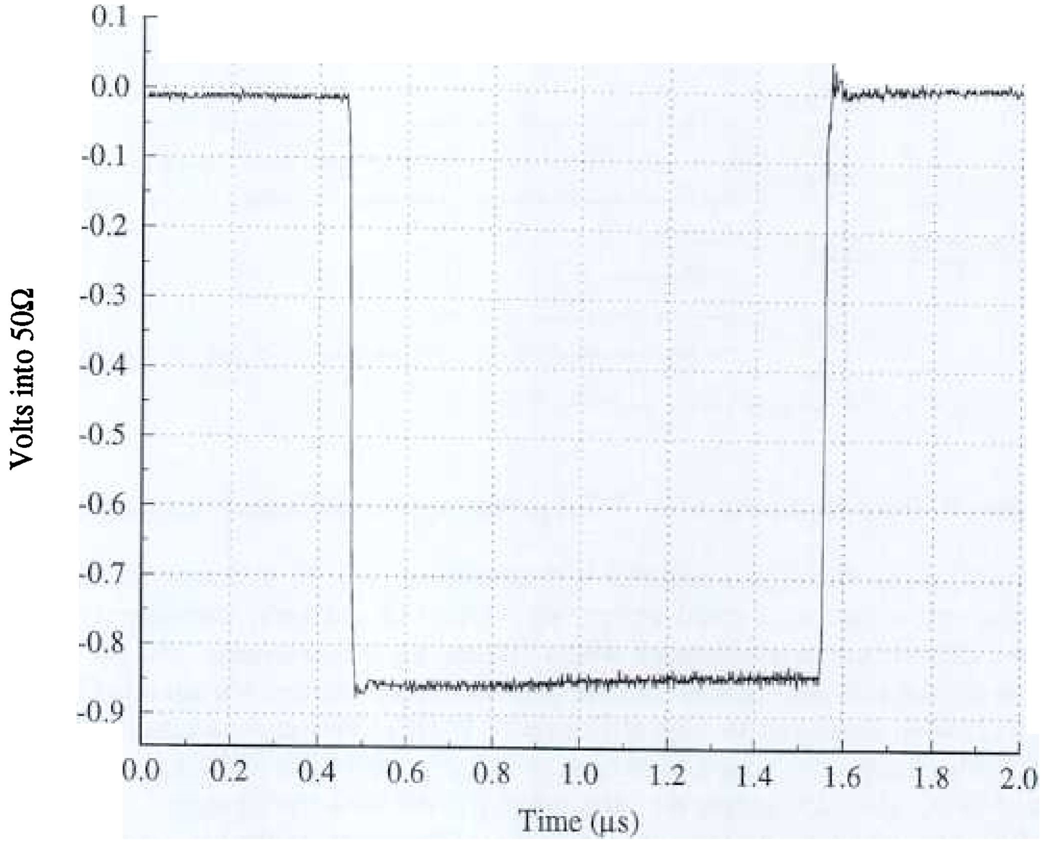

Figure 9 The output signal of the BCM for a test input pulse.

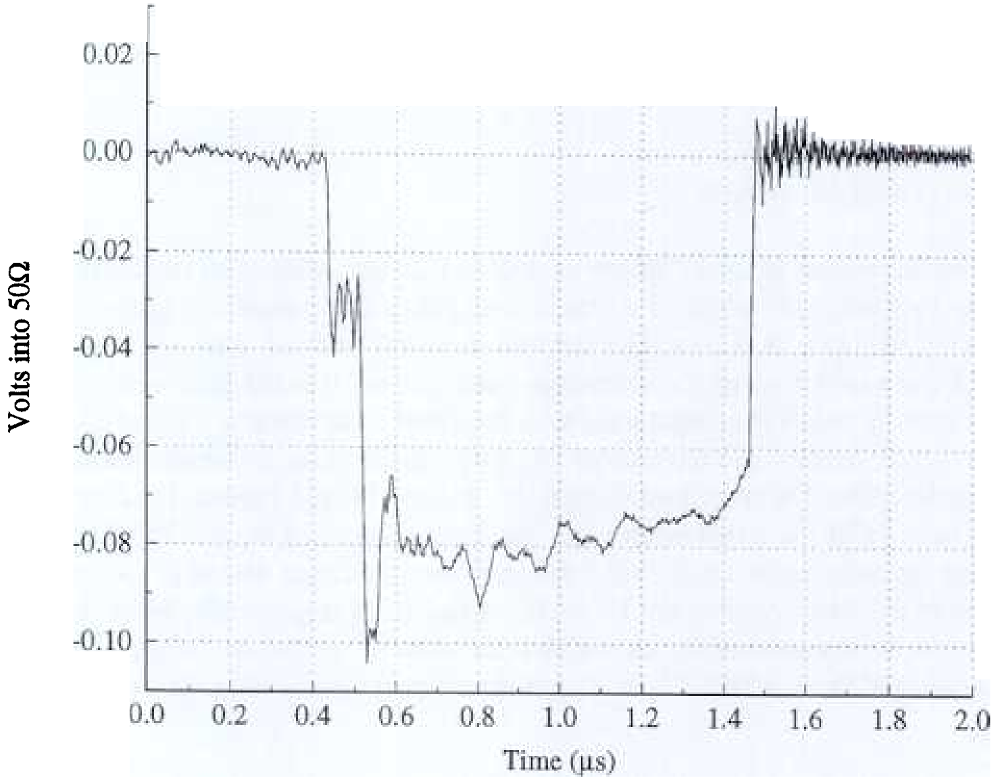

Figure 10 The output signal from the new BCM for a 1 μs beam pulse

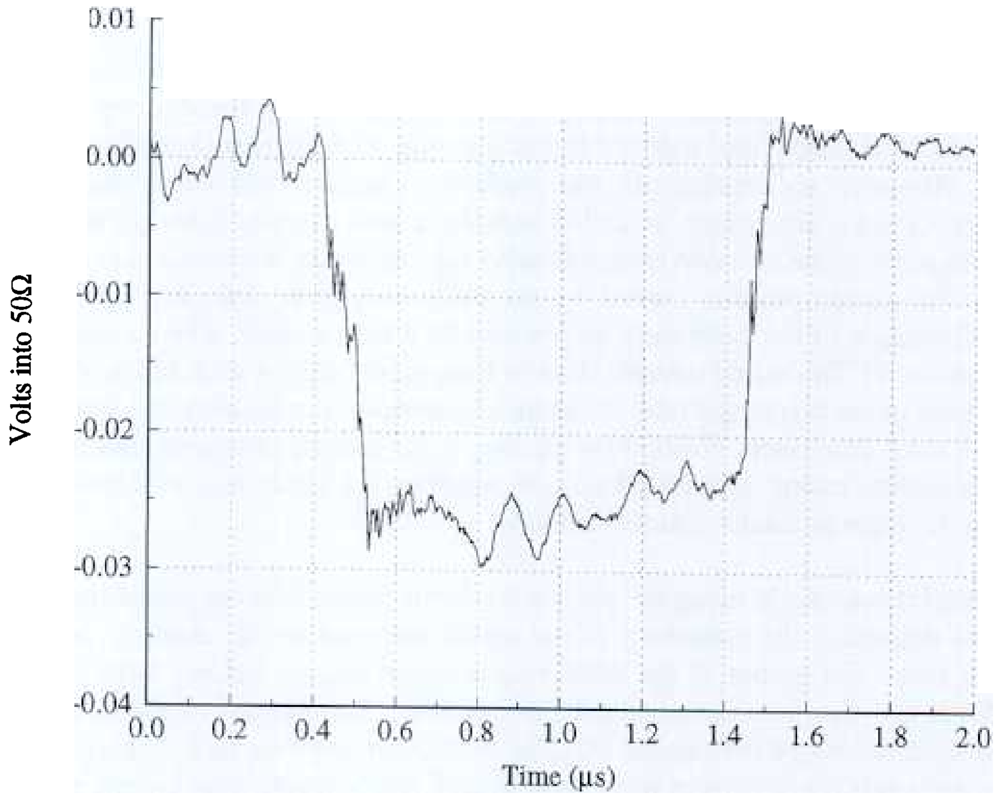

Figure 11 The output signal from the old BCM for a 1 μs beam pulse.

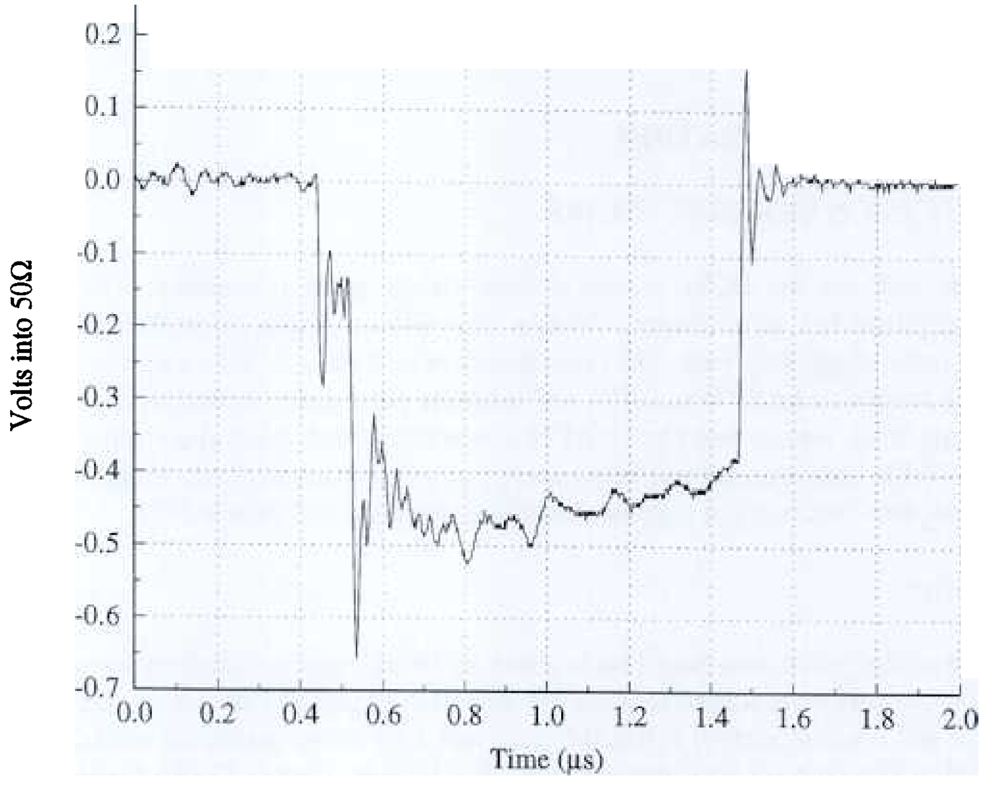

Figure 12 The charge collected from an aluminium target for a 1 μs beam pulse.

3.2 THE CALIBRATION LOOP

The calibration loop is provided to allow a calibration of the BCM response to a known pulsed current. One calibration procedure would be to use a high efficiency Faraday cup to measure the charge in an actual linac pulse, and then to compare this with the charge reading obtained from the ADC. However, no Faraday cup was available to make a calibration using this method. Instead a precision charge pulser is used to simulate a linac electron beam pulse. This happens to be a much easier procedure than using a Faraday cup, and it can be used to calibrate the system 'on-line'. The charge pulse is carried by the calibration loop, described earlier. The ideal position/orientation of the calibration loop would be a long straight wire running through the centre of the toroid. This would simulate the real linac pulse position well, but is not feasible due to the presence of the beam flight tube. An alternative position for the loop was investigated. The easiest and most convenient position for the loop is for a single closely wound turn within the toroid's aluminium casing, terminated so as to minimize the impedance mismatch between the cable from the pulse generator and the test loop.

A measurement was made using the precision current pulser with the calibration loop in this position to determine the sensitivity of the toroid response to the absolute position of the calibration loop. The output of the BCM was recorded using a LeCroy 9450 digital storage oscilloscope, and then transferred to a PC for analysis. The integral of the output pulse was calculated from the 'scope data on the PC. The calibration loop was then wound so that the net number of turns was zero (one turn was closely wound, one 'anti-turn' was loosely wound around the outer casing). The output pulse was again measured using the digital storage oscilloscope and its integral calculated. If the calibration loop is position-insensitive, then the output of the BCM for the 'turn plus anti-turn' should be small. The above measurements indicated that the 'turn anti-turn' arrangement cancelled each other out to 0.05% of the single turn response. This measurement was limited by the resolution of the LeCroy scope, the background noise pick-up, and the impedance mismatch of the precision current pulser to the single calibration loop. However, the insensitivity of the response to the position of this calibration loop was clearly demonstrated.

4 CHARGE CALIBRATION

4.1 PRECISION CURRENT PULSER

In order to calibrate the BCM, a well defined charge pulse is required. The best available commercial pulser has an accuracy of only ± 2%, and its output pulse does not simulate the accelerator pulse shape very well. The requirement at NPL was to have a current pulser with an output pulse known to better than 0.5%, and a similar pulse shape to that of the NPL linac. The main driving force was to use the BCM in conjunction with total absorption calorimetry to measure the NPL linear accelerator beam energy to an accuracy of better than ± 0.5%. In order to get the required accuracy, a current pulser was designed and built at NPL.

4.1.1 Design

The design of the pulser was based on a circuit by Dunn[3], and modified by Ross and Heistek[4]. This circuit was further modified to allow the selection of pulsed currents of size 2 to 62 mA in 2 mA steps, and nominal width 0.1, 0.2, 0.5, 1, 2, and 3 μs (these match the available accelerator pulse widths). The device was triggered by a + 6.6 V edge. **Figure 13** and **Figure 14** show the circuit diagrams for the current pulser and timing circuits respectively.

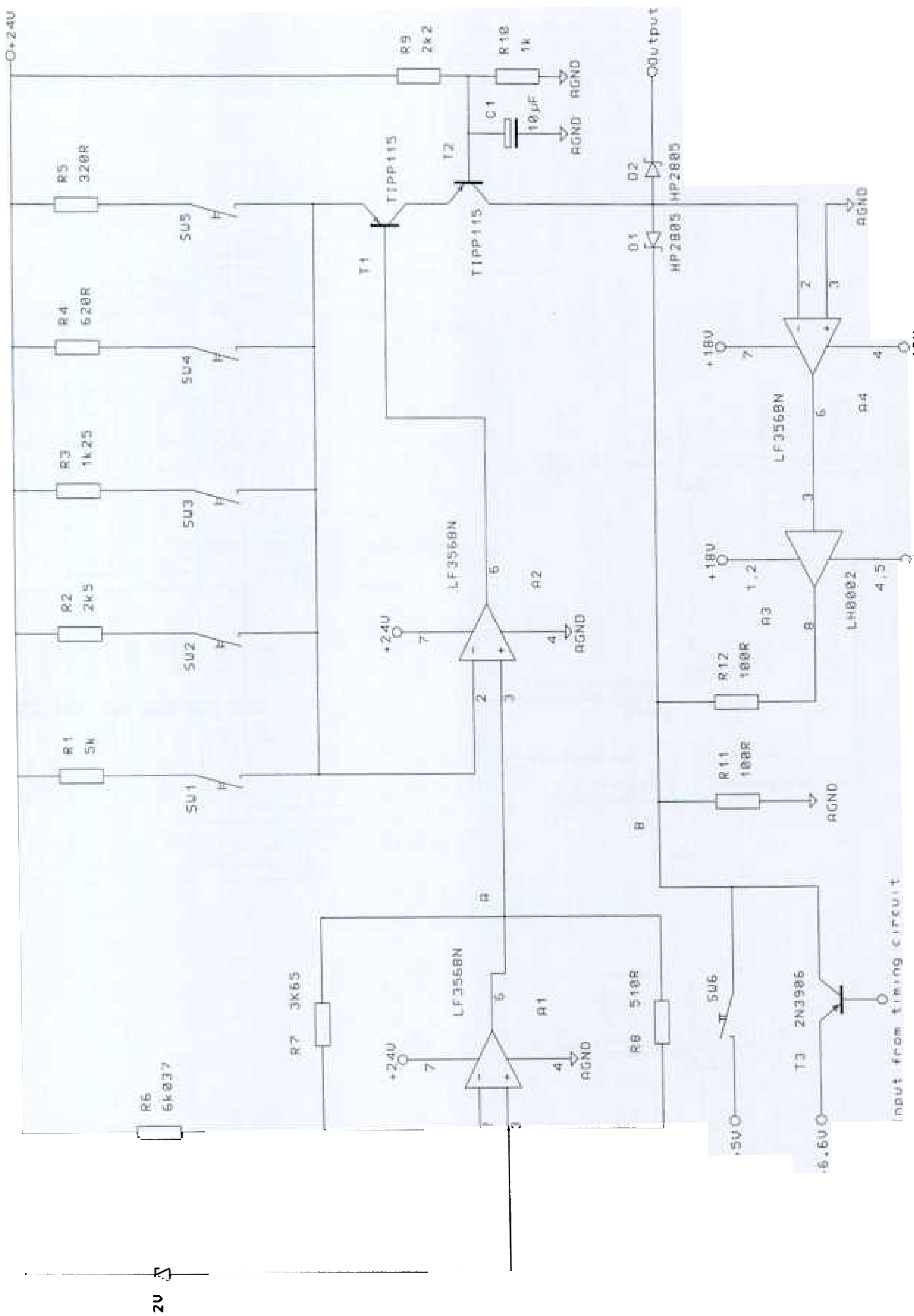

Figure 13 The current pulser amplitude circuit

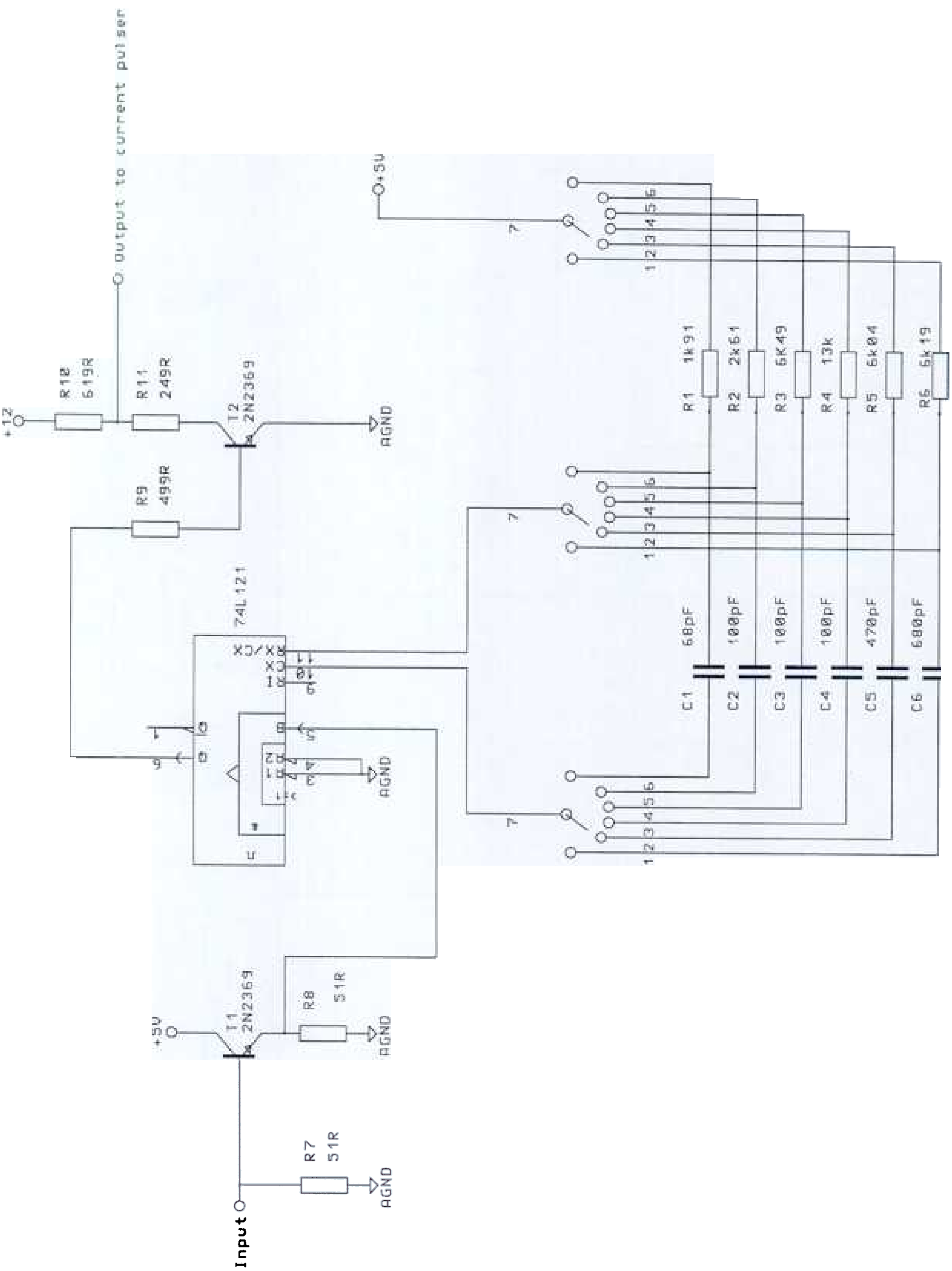

Figure 14 The pulse width timing circuit

4.1.2 Operating Principles

Op-amp A1 maintains the voltage at point A 10 V below the + 24 V supply rail. Op-amp A2, in conjunction with Darlington T1, maintains a voltage drop of 10 V across the resistors R1 to R5, thus forming a current source. Darlington T2 isolates the current source from transients in the fast diode gate. When transistor T3 is switched off, A3 and A4 maintain the output at zero volts, all the current being sunk by A3. When T3 is switched on, point B is raised to a potential of about + 6 V, reverse biasing diode D1, thus forcing all the current to flow through the output (this is only true for load a impedance such that the voltage generated across the load is less than 4.5 V).

The timing circuitry is based on a 74L121 flip-flop. Pulse widths are defined by resistors R1 to R6, and capacitors C1 to C6. The output of the 74L121 is only between 0 and 3.4 V, so it had to be boosted using a transistor to be between 0.6 and 12 V. This also helped to speed up the switch on/off time of the current pulser. There is also an override mode which switches to a DC output for currents of about 50 mA and less. The DC output stability was tested by measuring the voltage generated across an accurately known 51 Ω metal film resistor. The results are shown in **Figure 15**. The mean output varied by ± 0.03% (1 σ), with an absolute maximum variation of ± 0.08%.

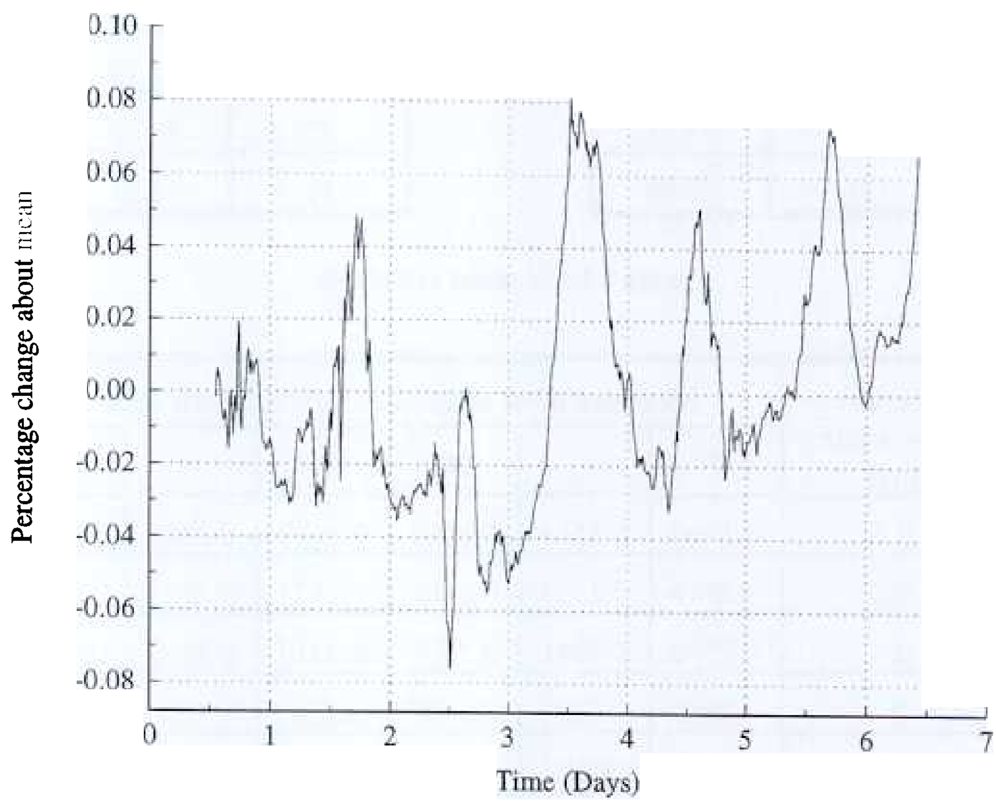

Figure 15 Stability of current pulser output switched to DC mode

4.1.3 DC Calibration

A DC calibration was made for currents between 2 and 52 mA, by measuring the voltage generated across a 51 Ω resistor. The results are shown in **Table 1. Table 2** shows the actual pulse widths measured for an output current of between 2 and 50 mA, as measured using a LeCroy 9450 digital storage oscilloscope, compared to the nominal values. The charge per pulse

Nominal current (mA)	Measured Current (mA)
2	1.720
4	3.637
6	5.584
8	7.577
10	9.591
12	11.59
14	13.60
16	15.74
18	17.75
20	19.76
22	21.77
24	23.78
26	25.79

Nominal current (mA)	Measured Current (mA)
28	27.80
30	29.82
32	30.94
34	32.98
36	34.98
38	37.00
40	39.01
42	41.02
44	43.04
46	45.05
48	47.19
50	49.21
52	51.21

Table 1 DC current calibration.

Nominal pulse width (μs)	Measured pulse width (μs) between 2 and 50 mA					
	2	10	20	30	40	50
0.1	0.1406	0.1518	0.1490	0.1417	0.1386	0.1391
0.2	0.2549	0.2533	0.2481	0.2433	0.2395	0.2352
0.5	0.5370	0.5291	0.5307	0.5310	0.5309	0.5310
1	1.049	1.065	1.068	1.068	1.068	1.068
2	2.026	2.041	2.044	2.044	2.043	2.044
3	3.007	3.022	3.024	2.024	3.024	3.024

Table 2 Measured pulse widths.

can be calculated by multiplying the DC current by the chosen pulse width, with an estimated accuracy of ± 0.25%

Measurements from pulsed calibrations have been compared and found to be stable to ± 0.2% (1 σ) over a period of one month.

4.2 CALIBRATION OF THE CURRENT PULSER

The precision current pulser is used to obtain an absolute charge calibration for the BCM/ADC. The following procedure describes how to calibrate the system to give maximum resolution for 1 μs beam pulses, and beam currents between 6 and 10 mA.

For maximum resolution, the LeCroy ADC should read full scale (i.e., about 2000 counts) at the maximum beam pulse current that is to be used. For pulses of 3 mA and greater (with a pulse width of 1 μs), the BCM output requires attenuation before being input to the ADC. The attenuation required can either be found by trial and error, or by using the following formula:

$$Attenuation(dB) = 20 \times log \left[\frac{I_b \times t_b}{} \times \frac{Z_d}{Z_a} \times \frac{G}{500 \times 10^{-12}} \right]$$

where I_b is the beam current in Amps, t_b is the beam pulse width in seconds, N is the turns ratio, Z_d is the differential amplifier input impedance in Ohms, Z_a is the ADC input impedance in Ohms, G is the gain of the differential amplifier, and 500×10^{-12} is the nominal maximum charge input to the ADC in coulombs. For a 10 mA, 1 μs beam pulse, this gives

$$Attenuation = 20 \times log \left[\frac{10mA \times 1\mu s}{24} \times \frac{100}{51} \times \frac{2}{500 \times 10^{-12}} \right] = 10.3\,dB$$

This attenuation should be increased by about ten percent to allow for the possibility of the linac output drifting upwards during a run.

For maximum accuracy, the current pulser should be calibrated shortly before use. The uncertainty on a calibration is about ± 0.05% (1 σ) over the period of several hours. The calibration is carried out using an electrometer[5] designed at NPL for the accurate measurement of ionization currents. The output of the current pulser is connected via URM 67 50 Ω coaxial cable to the input of the electrometer. The current pulser is then triggered n times, and the voltage generated across the electrometer's feedback capacitor measured (the number of pulses and the pulse repetition frequency (PRF) is chosen so that it is similar to the number of real beam pulses and the PRF used in an actual electron beam measurement). The charge per pulse for the current pulser can then be calculated from the formula

$$Charge per pulse = \frac{(V_c - V_{off}) \times C}{n}$$

where V_c is the voltage across the feedback capacitor C, and n is the number of pulses. V_{off} is the voltage recorded across the feedback capacitor for zero current pulses over the same integration period. **Table 3** shows the results of a typical 10 mA calibration of the current pulser for a 1 μs pulse, at a PRF of 40 Hz. The electrometer feedback capacitor C used was 498.98 nF, and the voltage offset correction V_{off} was - 0.0011 V.

V_c	n	$\frac{(V_c - V_{off}) \times C}{n}$
-3.9626	194	-1.0189e-8
-4.0445	198	-1.0190e-8
-4.1261	202	-1.0189e-8
-3.9833	195	-1.0190e-8
-4.0856	200	-1.0190e-8
-4.0853	200	-1.0190e-8
-4.1474	203	-1.0192e-8
-4.0650	199	-1.0190e-8
Mean charge per pulse = 1.0190e-8 C ± 0.007% (1 σ)		

Table 3 Pre-calibration of the current pulser

4.3 CALIBRATION OF THE BCM/ADC

The calibrated current pulser is then connected to the calibration loop of the toroid. The output of the BCM is connected to the ADC via the variable attenuator. The ADC is triggered by the controlling computer to find the ADC pedestal (The *pedestal* reading is the number of counts obtained when a gate pulse is applied to the ADC by the controlling computer with no analogue input pulse. It is a result of several factors, the largest of which is a charge injection by the ADC itself, the purpose of which is to assure proper ADC operation). The pulser is then triggered *n* times (*n* being chosen as before to match the number of real beam pulses and the PRF of a real electron beam measurement). The sum of all the *n* ADC readings is recorded by the computer. The response of the ADC to the input current pulse can be calculated using the formula

$$ADC = \left(\frac{Adcsum}{n} - Pedestal \right)$$

where *Adcsum* is the sum of the *n* ADC readings.

Table 5 shows the results of a typical calibration of the BCM/ADC for a 10 mA, 1 μs pulse at a frequency of 40 Hz. The pedestal in each case is the mean of 100 readings. The input attenuation was 12 dB(nom).

Following the BCM/ADC measurements, the current pulser is recalibrated using the electrometer to check for any drift in its output. **Table 4** shows the results of such a recalibration. In this instance the voltage offset V_{off} *was* -0.0013 V. The whole process is then repeated with different currents in the 6 to 10 mA range. A linear fit of the charge per pulse verses the ADC reading is made to get a calibration of the BCM/ADC. The result of a typical calibration is shown in **Figure 16**. It can be seen that the systems response is very linear, with the rms deviation being only 3.3 pC. Calibrations have been compared and found to be stable to ± 0.3% (1 σ) over the short term..

Pedestal	*n*	*Adcsum*	*ADC*
93.79	191	337412	1672.8
94.10	198	349925	1673.2
94.16	187	330516	1673.3
94.12	194	342838	1673.1
94.27	194	342897	1673.2
Mean ADC reading in counts = 1673.12 ± 0.01% (1 σ)			

Table 4 ADC/BCM charge calibration

V_c	*n*	$\frac{(V_c - V_{off}) \times C}{n}$
-3.9668	194	-1.0200e-8
-4.0073	196	-1.0199e-8
-3.9871	195	-1.0200e-8
-3.9666	194	-1.0199e-8
Mean charge per pulse = 1.0199e-8 C ± 0.003% (1 σ)		

Table 5 Post-calibration of the current pulser

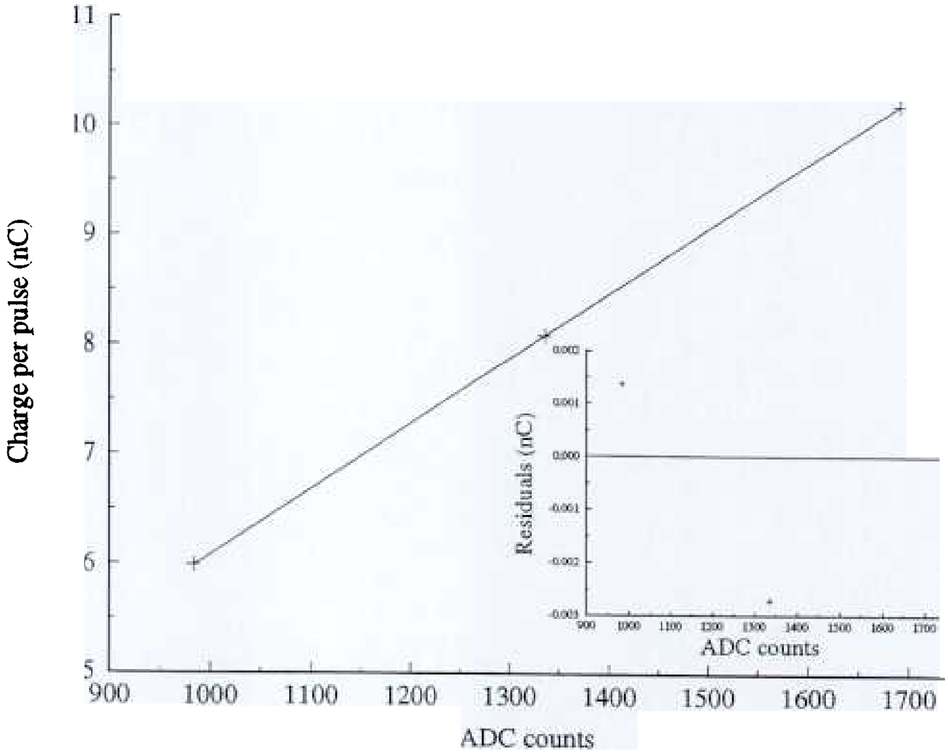

Figure 16 Calibration showing the beam charge against the number of ADC counts.

5 CONCLUSION

The new BCM is a significant improvement on the original beam current monitor, being faster and more sensitive, yet less susceptible to RF interference. The ability to calibrate the monitor in terms of the charge in the electron beam will significantly enhance electron dosimetry at NPL. For example, the calibration given in **Figure 16** was used in combination with total absorption calorimetry to determine the electron beam energy with an estimated accuracy of ± 0.5% (1 σ)[6]. This is significantly simpler and more accurate than other absolute methods of electron beam energy determination available at NPL.

6 REFERENCES

1. Burns, D.T. *An automated charge monitoring system for the NPL linear accelerator.* NPL Report RSA(EXT)80, August 1985

2. Sutter, D.F. *A wide band current monitor based on pulsed transformer techniques.* IEEE Transaction on Nuclear Science, **20, no.3**, June 1973, 665-7.

3. Dunn, P.C. *Absolute beam charge measurements with toroid monitors: experience at the Bates linac.* Nuclear Instruments and Methods **165**, 163

4. Ross, C. and Heistek, L. Private communication. National Research Council of Canada.

5. Sanders, R.P. *The design and operation of a high quality two-channel electrometer.* NPL Report RS(INT)106, January 1989

6. Williams, A.J. *Measurement of the NPL Linear Accelerator Beam Energy by totally Absorbing Calorimetry.* MSc Radiation Physics, University College London, 1994